Available online at www.sciencedirect.com
SCIENCE DIRECT
Journal of Power Sources 153 (2006) 239–244
JOURNAL OF POWER SOURCES
www.elsevier.com/locate/jpowsour

Influential factors on oxygen reduction at $La_{1-x}Ca_xCoO_3$ electrodes in alkaline electrolyte

Abderrezak Hammouche [a,*], Abdelkrim Kahoul [b], Dirk Uwe Sauer [a], Rik W. De Doncker [a]

[a] *Electrochemical Energy Conversion and Storage Systems Group, Institute for Power Electronics and Electrical Drives, Aachen University of Technology, Jägerstrasse. 17-19, D-52066 Aachen, Germany*
[b] *Laboratory for Energetics and Electrochemistry of Solids, Department of Process Engineering, F. Abbas University of Setif, DZ-19000 Setif, Algeria*

Available online 7 July 2005

Abstract

Reduction of oxygen was investigated on porous electrodes made of $La_{1-x}Ca_xCoO_3$ (with $0 \leq x \leq 0.6$) perovskite-structured oxides, prepared by a sol–gel process. It was found that both the reaction rate and the electrode active surface area (determined by cyclic voltammetry in a narrow capacitive potential range and by impedance spectroscopy) depend on the partial substitution ratio x, both displaying a maximum value for x nearly equal to 0.4. However, in spite of the parallel trend exhibited by the reduction current and the electroactive surface area parameter, the current varies much more with x, that is, while the change in the surface area amounts to approximately 40% over the explored x range, the current increases fivefold. Subsequent investigation of the electrode surface composition revealed that surface cobalt concentration (estimated by XPS analysis) deviates significantly from the nominal bulk composition (determined by EDX analysis). It follows a similar dependence on x, showing equally a maximum for x near to 0.4. Such a behaviour seems to have a greater effect on the reaction rate, since Co cations are the surface active sites for oxygen electro-reduction.

Keywords: Perovskite-type cobalt oxide; Oxygen reduction; Surface area; Surface composition

1. Introduction

Electro-reduction of oxygen on perovskite-structured oxides is of considerable importance for numerous electrochemical devices such as alkaline and solid-oxide fuel cells, and secondary metal-air batteries. Mixed lanthanum and cobalt-based oxides appear to be promising air electrodes not only for the oxygen evolution [1] but for its reduction as well [2,3], and can thus be used simultaneously as bifunctional electrode [4–7].

In a previous investigation [8], we showed that $La_{1-x}Ca_xCoO_3$ oxides ($0 \leq x \leq 0.6$), prepared by a sol–gel process using propanol as synthesis medium, exhibited better electrochemical activity towards oxygen reduction and evolution over their counterparts prepared using water as synthesis medium. Such a performance was basically related with their single-phase formation, grain-to-grain chemical homogeneity and good electrical conductivity, which all closely depended on the partial substitution ratio x of La with Ca. Within the $La_{1-x}Ca_xCoO_3$ series, the electroactivity and specific surface area (S_{BET}) features exhibited similar dependence on x, both passing through a maximum for x nearly equal to 0.4. Although the geometric effect of the electrode surface was minimised by using plain electrodes, the pores of which have been deliberately obstructed, the reduction current still strongly depended on the calcium substitution degree x. This indicates that other physicochemical features of the electrode material have a primary influence on the reaction kinetics.

In the present work, we investigate the electrochemical behaviour of such electrodes prepared in the porous form. We evaluate their actual surface area involved in the interfacial reaction, on the one hand, and look into other parameters,

* Corresponding author. Tel.: +49 241 80 969 73; fax: +49 241 80 92203.
E-mail address: hm@isea.rwth-aachen.de (A. Hammouche).

0378-7753/$ – see front matter © 2005 Elsevier B.V. All rights reserved.
doi:10.1016/j.jpowsour.2005.05.028

such as the electrode surface composition, which possibly have a significant influence on the reaction kinetics, on the other hand.

2. Experimental

2.1. Materials

Ca-doped lanthanum cobaltites ($La_{1-x}Ca_xCoO_3$ with $0 \leq x \leq 0.6$) samples were synthesized following the amorphous citrate precursor method described in [8], using propanol as solvent. According to the microscopic investigation and X-ray diffraction analysis [8], all compounds were found to be single-phased occurring in a perovskite structure.

2.2. Characterisation methods

The samples specific surface area (S_{BET}) was measured on powders by the BET method using a Perkin-Elmer Shell Sorptometer.

Electrochemical measurements were carried out using a three-electrode set-up in 1 M KOH electrolyte solution. Porous working electrodes were obtained by moderately pressing $La_{1-x}Ca_xCoO_3$ powder in form of thin cylindrical pellet (1 cm^2 base surface area) for 1 min at 1 t cm^{-2}. Only one face of the pellet was exposed to the electrolyte, the remaining surface, including a copper wire electrical contact, was isolated with Araldite. A platinum foil and an Hg/HgO electrode, in the same potassium hydroxide concentration as the cell electrolyte, were employed as counter- and reference electrodes, respectively. The solution was gently stirred during the experiments by means of a magnetic stirrer. The temperature of the experiments was equal to $23 \pm 1\,^{\circ}C$. Polarisation and impedance measurements were performed using an Autolab PGStat30. Impedance spectra were recorded in the 10^5 to 10^{-2} Hz range with an ac signal of 10 mV amplitude.

Quantitative determination of La, Ca and Co elemental concentrations both in the bulk and at the surface of the samples was performed respectively by means of energy-dispersive X-ray spectroscopy (EDX) and X-ray photoelectron spectroscopy (XPS). XPS analysis was conducted using an Al X-ray source. Curve fitting was performed on the basis of Gaussian peaks and binding energies (BE) were determined with reference to the C 1s signal.

3. Results and discussion

3.1. Electrochemical behaviour

The electrochemical behaviour of $La_{1-x}Ca_xCoO_3$ electrodes for oxygen reduction was investigated by plotting current–overpotential curves in the steady-state regime. The open-circuit potentials ranged between 0.05 and 0.2 V versus Hg/HgO, the solution being in contact with air. Fig. 1 confirms the expected dependence of the current on the substitution degree x, exhibiting particularly a maximum activity at x close to 0.4, as previously observed with $La_{1-x}Ca_xCoO_3$ flat surface electrodes, the pores of which have been deliberately obstructed using polystyrene solution [8]. By way of illustration, Fig. 2 shows the cathodic current obtained at overpotentials of −0.3 and −0.5 V for the different compositions. Quantitatively, the reduction current recorded with the present porous electrodes is nearly two orders of magnitude larger than that corresponding to the flat surface electrodes, stressing that the reaction basically takes place on top of the internal surface of the electrode pores.

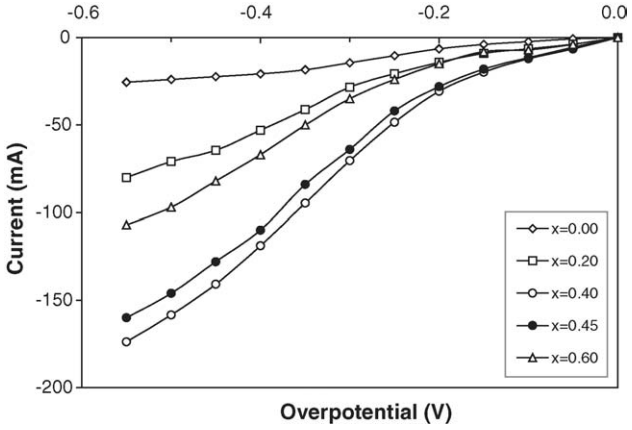

Fig. 1. Current–overpotential curves of oxygen reduction on porous $La_{1-x}Ca_xCoO_3$ pellets, in 1 M KOH at 23 °C.

3.2. BET surface area, S_{BET}

One of the main advantages of the solution preparative techniques is the grain fineness, which yields samples with considerably developed surface area and, accordingly, with improved electrode kinetics. Fig. 3 displays the evolution of BET surface area with the degree of lanthanum substitution x.

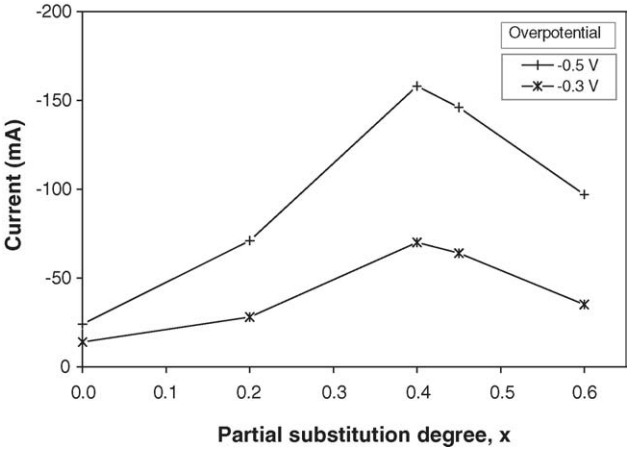

Fig. 2. Electrode performance for oxygen reduction as a function of x at −0.3 and −0.5 V overpotential.

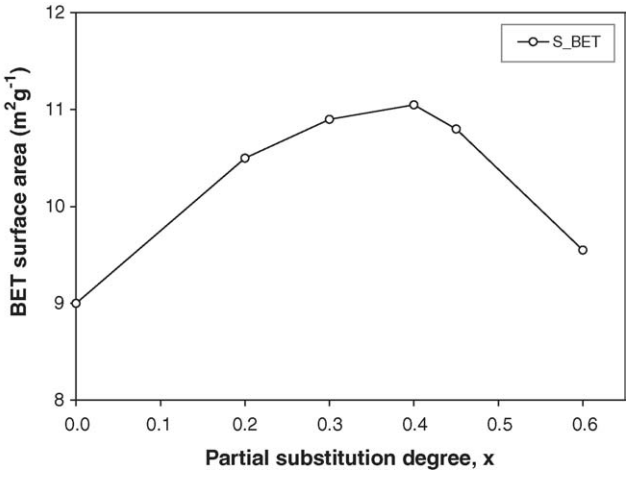

Fig. 3. Specific surface area dependence on calcium content x for $La_{1-x}Ca_xCoO_3$ samples.

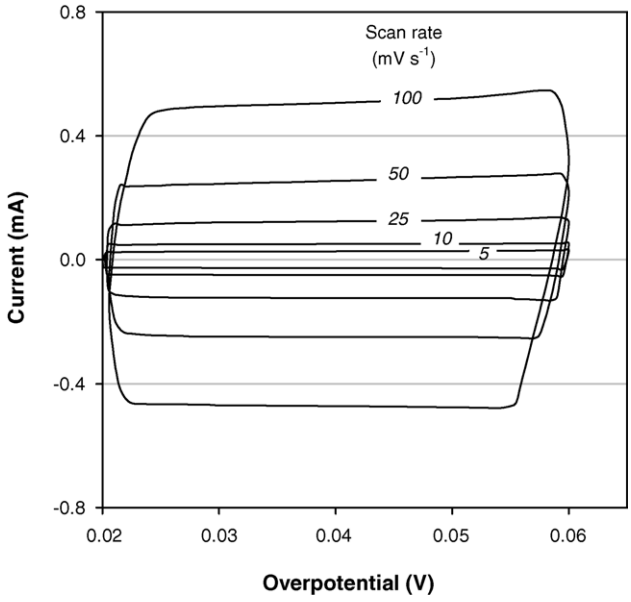

Fig. 4. Cyclic voltammograms of $LaCoO_3$ electrode in the 0.02–0.06 V overpotential range, in 1 M KOH at 23 °C.

As a result of the evolution of the average particle size with x [8], this parameter increases monotonously up to $x = 0.4$, then decreases for higher x values. This trend is similar to that exhibited by the evolution of the oxygen reduction current with x (cf. Fig. 2). The S_{BET} values obtained here have the same order of magnitude of those reported elsewhere [6,9].

3.3. Determination of the electrode active surface area from voltammetric curves, S_{vol}

Obviously, the actual electrode surface area, which affects the electrode kinetics, is only the surface of the compacted porous electrode exposed to the electrolyte. A first attempt to determine this parameter was made by measuring the double-layer charging current within a narrow potential range where the faradaic processes can be regarded as negligible. Fig. 4 shows typical cyclic voltammograms recorded at varying sweep rates in the 0.02–0.06 V overpotential interval. All curves exhibit quite symmetrical horizontal plateaus for the scan rates used.

The double-layer capacitance C_{dl} values were evaluated from the slope of the linear plots "$\Delta i_{cap} = i_a - i_c$", where i_a and i_c denote respectively the anodic and cathodic currents measured at the middle of the potential range, as a function of scan rate (Fig. 5). Note that using the difference Δi_{cap}, rather than the individual values of i_a or i_c, eliminates most of the error due to any faradaic current in the calculation of C_{dl}.

The actual surface area, S_{vol}, of the electrodes was then computed assuming a value of 60 μF cm^{-2} for C_{dl}, according to the view of Levine and Smith [10] for a perfectly flat oxide/electrolyte interface. Fig. 6 displays the variations of the electroactive surface area, referred to 1g, for the different electrode compositions. Although the surface area exposed to the electrolyte, S_{vol}, is approximately two orders of magnitude smaller than that determined on powders by the BET method (cf. Fig. 3), the curve also shows an increase in this parameter with the calcium content, reaching a maximum for $x = 0.45$. S_{vol} values increase by roughly 40% when the composition parameter x passes from 0 to 0.45.

3.4. Determination of the electrode active surface area by impedance measurements, S_{imp}

de Levie [11] developed a simple ac signal theory for porous electrodes in the absence of dc current, relating their ac behaviour to that of a corresponding planar electrode. For a system with semi-infinite cylindrical pores, the apparent impedance Z_p of the pore interface is given by

$$Z_p = (ZR)^{1/2} \coth(l/\lambda) \quad (1)$$

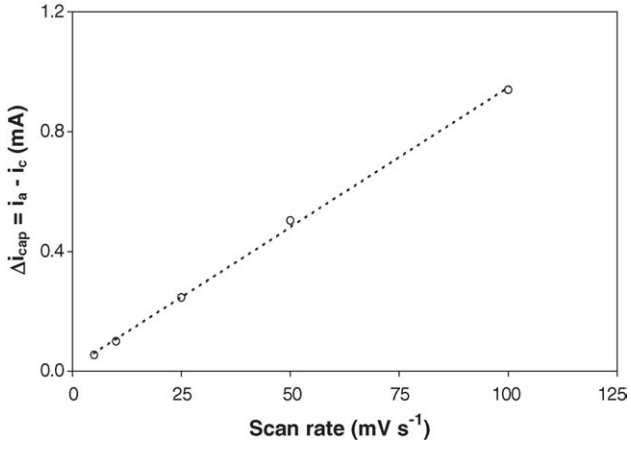

Fig. 5. Linear variations of "$\Delta i_{cap} = i_a - i_c$" vs. scan rate for $LaCoO_3$ electrode, with i_a and i_c denoting respectively the anodic and cathodic currents measured at the middle of the potential range in Fig. 4.

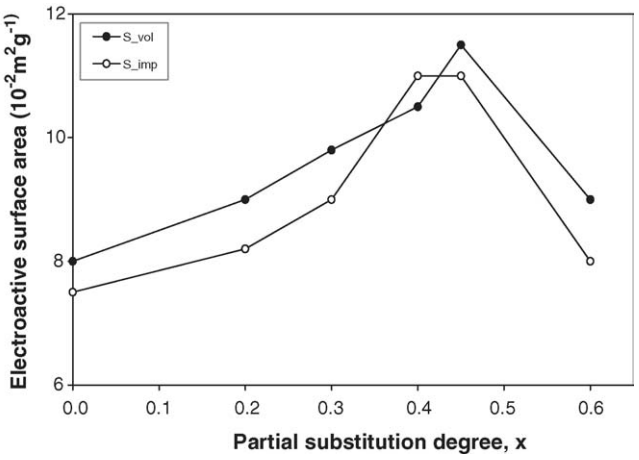

Fig. 6. Variations of the electroactive surface area, determined both from the voltammetric capacitive currents, S_{vol}, and the impedance diagrams, S_{imp}, as a function of electrode composition.

with

$$\lambda = (Z/R)^{1/2} \quad (2)$$

where Z and R are respectively the impedance and ohmic resistance of the pore per unit length, l the pore length and λ is the penetration depth of the ac signal. The porous behaviour is expected for the electrode at higher frequencies as long as the penetration depth of the ac signal is smaller than the pore length ($\lambda \ll l$). In this case, Eq. (1) simplifies to

$$Z_p = (ZR)^{1/2} \quad (3)$$

Accordingly, since the resistance R behaves as a scalar, the absolute magnitude of the impedance is proportional to the square root of the corresponding planar electrode impedance, whilst the phase angle is half that of the equivalent flat electrode. As the frequency decreases, the interfacial impedance increases compared to the pore ohmic resistance, making the signal penetration depth increase and ultimately overrun the entire pore length ($\lambda \gg l$). In this case, the electrode behaves as a flat electrode and its impedance becomes

$$Z_p = Z/l \quad (4)$$

The transition porous-planar behaviour occurs at a specific frequency at which the ohmic resistance of the pore becomes equal to its interfacial impedance.

If we consider the capacitive-only situation corresponding to double-layer charging, as is the case of the systems under study, the interfacial impedance Z is given by

$$Z = -j/\omega C_{dl} \quad (5)$$

where $j = (-1)^{1/2}$, ω is the angular frequency and C_{dl} is the double-layer capacitance. The Nyquist impedance plot is expected to exhibit a linear increase with a phase angle of 45° at high frequencies, switching to a vertical line to the real axis at frequencies lower than the critical value. Combination of Eqs. (3) and (5) predicts an equal and linear dependence

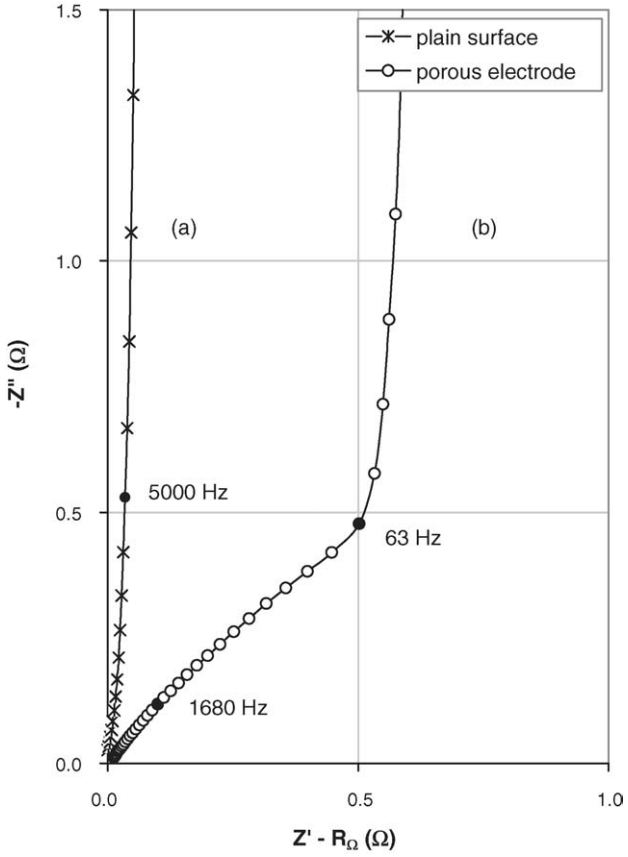

Fig. 7. Complex plane impedance plots at the open-circuit potential for (a) flat surface and (b) porous $La_{0.6}Ca_{0.4}CoO_3$ electrodes, in 1 M KOH at 23 °C.

both of the impedance real and imaginary components versus $\omega^{-1/2}$ in the high frequency domain.

Impedance measurements were performed at the open-circuit potential, where no significant faradaic reaction is taking place. Nyquist plots (a) and (b) in Fig. 7 correspond respectively to plain and porous $La_{0.6}Ca_{0.4}CoO_3$ mixed oxide electrode, after deduction of the ohmic resistance (R_Ω) of the free electrolyte solution. The linear quasi-vertical shape of spectrum (a), observed over the whole frequency range, unambiguously describes a planar behaviour for this electrode. A value of approximately 51 μF cm^{-2} has been estimated for the double-layer capacitance according to Eq. (5). This value compares well with that usually taken into account for oxide-based electrodes, estimated at 60 μF cm^{-2} [10]; the difference may be ascribed to some reduction in the outer surface area resulting from pore filling with polystyrene. Spectrum (b) displays a typical diagram obtained on porous pellet electrodes. Two distinct linear domains appear on this spectrum: a high frequency range (>63 Hz), exhibiting an almost 45° phase angle, describing the porous character of the electrodes, and a low frequency one (<63 Hz), where the impedance branch is virtually a vertical line, corresponding to their planar character. The variations of both of the imaginary and real impedance parts in the high frequency domain were checked to be almost equal and display a linear dependence

on $\omega^{-1/2}$, supporting the approach of the cylindrical-shaped pore model adopted for these electrodes.

The actual electrode surface area, S_{imp}, can be estimated knowing the electrode capacitance and the unit surface capacitance values. The former is determined from the impedance imaginary component of the vertical branch. When the frequency decreases, the C_{dl} value increases slightly, and reaches a limit. Fig. 6 depicts the variations of S_{imp} parameter with the sample substitution degree x. S_{imp} values derived from the impedance measurements match those deduced from voltammetric curves, also showing a close dependence on x with a maximum value at x between 0.4 and 0.45.

The variations of the electrode surface area values show the same tendency with x, like those of the reduction current presented in Section 3.1. However, it is important to point out that while the change in the surface area amounts to ca. 40% over the explored substitution range, the reaction current increases by a factor of nearly 5. It seems thus that the increase in the current is not merely due to the effect of the surface area factor, but likely to another more effective parameter which controls the electrode activity.

3.5. Analysis of the electrode surface composition

Since oxygen electro-reduction is an interfacial process, we performed a surface analysis by means of XPS technique in order to disclose a possible relationship between the reaction rate and the surface states. Fig. 8 shows two survey spectra for $La_{1-x}Ca_xCoO_3$ electrodes with $x = 0$ and 0.4. The latter is a representative spectrum for all calcium-containing samples. The characteristic lines for lanthanum, cobalt, calcium and oxygen were identified in reference to literature data [12–16].

The La 3d spectrum consists of two doublets situated at binding energy of 835.5 and 838.7 eV. The Co $2p_{3/2}$ signal gives an asymmetrical peak typical of Co^{3+} ions at 780.6 eV. The O 1s spectrum can be deconvoluted in three peaks: the one with lower BE (529.4 eV) is assigned to lattice oxygen, the next (531.6 eV) is ascribed to hydroxyl group or adsorbed oxygen and the third peak (532.9 eV) is due to moisture. It can be noticed that the peak area corresponding to oxygen in

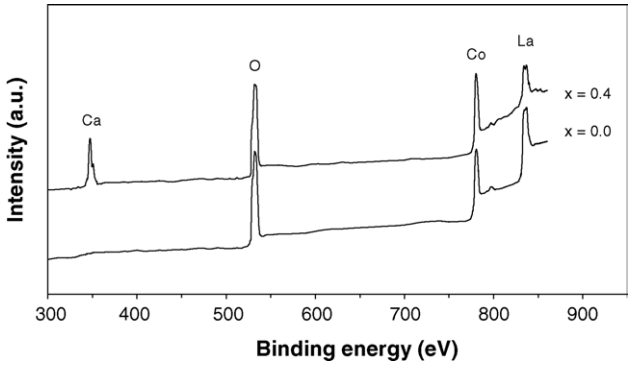

Fig. 8. Survey XPS spectra of the $La_{1-x}Ca_xCoO_3$ series perovskite oxides.

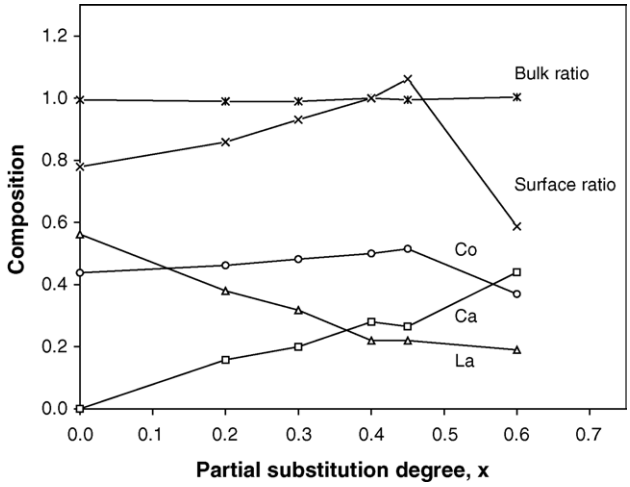

Fig. 9. Surface metal composition and atomic ratio (Co/(La + Ca)) in the bulk and at the surface (note that the sum of surface metal fractions is taken equal to 1).

the lattice decreases with x increasing, in accordance with the increase in oxygen sub-stoichiometry, which has been determined by chemical analysis in a previous study [8]. The Ca 2p signal gives two peaks $2p_{3/2}$ and $2p_{1/2}$ centred respectively at 347.2 and 350.8 eV.

The surface composition of the various elements is depicted in Fig. 9. In contrast to the homogeneous distribution of all cations in the material bulk, observed by EDX analysis, the XPS results reveal that surface metal concentrations deviate significantly from the expected nominal values. Such a behaviour, commonly reported for homologous multicomponent catalyst systems, is likely due to the difference in the surface tension of the various elements [17]. It is important to note that the surface cobalt content, deficient at lower x values, increases gradually with x increasing up to the stoichiometric ratio for $x = 0.45$, then drops. Because of the fact that the reactivity of perovskite is attributed to the active transition metal B ion in ABO_3 mixed oxides, the atomic ratio of B/A (where B = Co and A = La + Ca) can be considered as an index representing the catalyst activity [12,13]. Fig. 9 also indicates that this ratio possesses a maximum value lying near to 0.45. This shape of curve has also been reported for Mn-, Ni- and Co-based perovskite oxides investigated as catalysts for methane and CO oxidation [12] and NO reduction [13], each showing a maximum at a specific x value.

It is of particular importance to point out the parallel trend of the oxygen electro-reduction rate (Fig. 2) and the evolution of the surface cobalt concentration (Fig. 9), displaying simultaneously the highest values of electroactivity for oxygen reduction and Co/(La + Ca) ratio at a value of x lying between 0.4 and 0.45. Such a correlation evinces the key role of the surface concentration of the Co cations as active sites in the reaction kinetics. Indeed, it is known [18] that, before charge transfer occurs, oxygen reduction involves an adsorption process which proceeds through either “end-on”

configuration (i.e., O_2 molecule adsorbs by one oxygen atom) or "bridge" mechanism (i.e., O_2 molecule adsorbs by both atoms), depending on the distance between the surface active centres (compared to O–O bond distance) and on their concentration. The latter mechanism corresponds to easier O–O bond splitting and hence favours the reduction kinetics. Thus, an increase in the surface Co concentration may have an important effect inasmuch as it increases the number of surface active centres which would promote the "bridge"-type adsorption.

4. Conclusions

This work was undertaken for the purpose to elucidate the influence of physicochemical parameters of $La_{1-x}Ca_xCoO_3$ porous electrodes on the rate of oxygen reduction. Within this series, it was observed that the electrode material having an x value of 0.4 shows the maximum activity. The electrode surface area (determined consistently by means of two different electrochemical methods) was found to exhibit a similar dependence on x. However, from a quantitative viewpoint, it could not explain the huge increase of the current with the electrode composition, indicating the involvement of another much more effective parameter. By the application of XPS technique, it has been possible to analyse the chemical composition of the surface. This revealed a deviation from its bulk composition, particularly for the concentration of Co cations, showing a dependence on x similar to that of the reaction rate. The increase in the surface Co concentration seems to have a major effect on speeding up the electrode kinetics. Such a result suggests the feasibility of further enhancing the electrode activity by deliberate adding of cobalt; a statement which requires further examination in a future work.

References

[1] R.N. Singh, S.K. Tiwari, T. Sharma, P. Chartier, J.-F. Koenig, J. New Mater. Electrochem. Syst. 2 (1999) 65.
[2] V. Hermann, D. Dutriat, S. Müller, Ch. Comninellis, Electrochim. Acta 46 (2000) 365.
[3] X. Wang, P.J. Sebastian, M.A. Smit, H. Yang, S.A. Gamboa, J. Power Sources 124 (2003) 278.
[4] Y. Shimizu, K. Uemura, H. Matsuda, N. Miura, N. Yamazoe, J. Electrochem. Soc. 137 (1990) 3430.
[5] S. Müller, K. Striebel, O. Haas, Electrochim. Acta 39 (1994) 1661.
[6] M. Bursell, M. Pirjamali, Y. Kiros, Electrochim. Acta 47 (2002) 1651.
[7] D. Chartouni, N. Kuriyama, T. Kiyobayashi, J. Chen, J. Alloys Compd. 330–332 (2002) 766.
[8] A. Kahoul, A. Hammouche, F. Nâamoune, P. Chartier, G. Poillerat, J.-F. Koenig, Mater. Res. Bull. 35 (2000) 1955.
[9] N.-L. Wu, W.-R. Liu, S.-J. Su, Electrochim. Acta 48 (2003) 1567.
[10] S. Levine, A.L. Smith, Discuss. Faraday Soc. 52 (1971) 290.
[11] R. de Levie, in: P. Delahay (Ed.), Advances in Electrochemistry and Electrochemical Engineering, vol. VI, Interscience, New York, 1967, p. 329.
[12] K. Tabata, I. Matsumuto, S. Kohiki, J. Mater. Sci. 22 (1987) 1882.
[13] S.-T. Shen, H.-S. Weng, Ind. Eng. Chem. Res. 37 (1998) 2654.
[14] R.H.E. van Doorn, H.J.M. Bouwmeester, A.J. Burgraaf, Solid State Ionics 111 (1998) 263.
[15] M. O'Connell, A.K. Norman, C.F. Hüttermann, M.A. Morris, Catal. Today 47 (1999) 123.
[16] Ph. Decorse, G. Caboche, L.-C. Dufour, Solid State Ionics 117 (1999) 161.
[17] S.H. Overbury, P.A. Bertrand, G.A. Somorjai, Chem. Rev. 75 (1975) 547.
[18] P.R. Adžić, J.X. Wang, Electrochim. Acta 45 (2000) 4203.